Available online at www.sciencedirect.com
ScienceDirect
Journal of Molecular Catalysis A: Chemical 271 (2007) 261–265
JOURNAL OF MOLECULAR CATALYSIS A: CHEMICAL
www.elsevier.com/locate/molcata

A synergistic effect of α-$Bi_2Mo_3O_{12}$ and γ-Bi_2MoO_6 catalysts in the oxidative dehydrogenation of C_4 raffinate-3 to 1,3-butadiene

Ji Chul Jung [a], Howon Lee [a], Heesoo Kim [a], Young-Min Chung [b], Tae Jin Kim [b], Seong Jun Lee [b], Seung-Hoon Oh [b], Yong Seung Kim [b], In Kyu Song [a,*]

[a] *School of Chemical and Biological Engineering, Institute of Chemical Processes, Seoul National University, Shinlim-dong, Kwanak-ku, Seoul 151-744, South Korea*
[b] *SK Corporation, Yuseong-ku, Daejeon 305-712, South Korea*

Received 22 January 2007; accepted 6 March 2007
Available online 12 March 2007

Abstract

α-$Bi_2Mo_3O_{12}$ and γ-Bi_2MoO_6 catalysts were prepared by a co-precipitation method for use in the oxidative dehydrogenation of C_4 raffinate-3 to 1,3-butadiene. A series of mixed catalysts composed of α-$Bi_2Mo_3O_{12}$ and γ-Bi_2MoO_6 were also prepared by a mechanical mixing method to investigate any synergistic effects of α-$Bi_2Mo_3O_{12}$ and γ-Bi_2MoO_6 catalysts in the oxidative dehydrogenation of C_4 raffinate-3. The α-$Bi_2Mo_3O_{12}$ and γ-Bi_2MoO_6 catalysts were formed successfully, as confirmed by XRD, FT-IR, Raman spectroscopy, and ICP-AES analyses. The γ-Bi_2MoO_6 catalyst exhibited a better catalytic performance than the α-$Bi_2Mo_3O_{12}$ catalyst due to its facile oxygen mobility. The conversion of n-butene and the yield for 1,3-butadine over the mixed catalysts showed volcano-shaped curves with respect to γ-Bi_2MoO_6 content due to the synergistic effect of the α-$Bi_2Mo_3O_{12}$ and γ-Bi_2MoO_6 catalysts. Among the mixed catalysts, the catalyst composed of 10 wt.% α-$Bi_2Mo_3O_{12}$ and 90 wt.% γ-Bi_2MoO_6 showed the best catalytic performance. The γ-Bi_2MoO_6 catalyst retained a higher oxygen mobility than the α-$Bi_2Mo_3O_{12}$ catalyst, while the α-$Bi_2Mo_3O_{12}$ catalyst retained much more adsorption sites for *n*-butene than the γ-Bi_2MoO_6 catalyst. The synergistic effect of the α-$Bi_2Mo_3O_{12}$ and γ-Bi_2MoO_6 catalysts in the oxidative dehydrogenation of C_4 raffinate-3 was due to a combination of the facile oxygen mobility of γ-Bi_2MoO_6 and the abundant adsorption sites of α-$Bi_2Mo_3O_{12}$ for *n*-butene.

Keywords: Bismuth molybdate; C_4 raffinate-3; 1,3-Butadiene; Oxidative dehydrogenation; Synergistic effect; Oxygen mobility; Adsorption ability

1. Introduction

The oxidative dehydrogenation of *n*-butene has attracted considerable interest as a promising process for producing 1,3-butadiene in a single unit [1–3]. The oxidative dehydrogenation of *n*-butene is independent of the naphtha cracking unit in the production of 1,3-butadiene in the sense that no additional major naphtha cracking products such as ethylene and propylene are produced in the production of 1,3-butadiene [2–5]. Furthermore, the oxidative dehydrogenation of *n*-butene has many advantages over the conventional naphtha cracking process in producing 1,3-butadiene. For example, the commercial value of C_4 raffinate-3 can be maximized by producing 1,3-butadiene through an oxidative dehydrogenation reaction. C_4 raffinate-3 is a residue obtained after separating 1,3-butadiene, isobutene, and 1-butene from the C_4 raffinate stream in a naphtha cracking unit. C_4 raffinate-3, therefore, is mainly composed of 2-butene (*trans*-2-butene and *cis*-2-butene), *n*-butane, and unseparated 1-butene.

Bismuth molybdates have been widely investigated as efficient catalysts for the oxidative dehydrogenation of *n*-butene [6–8]. Typically, three types of bismuth molybdates, α-$Bi_2Mo_3O_{12}$, β-$Bi_2Mo_2O_9$, and γ-Bi_2MoO_6, have been considered for this reaction [9–11]. However, it has been reported that β-$Bi_2Mo_2O_9$ is thermally unstable and decomposes into α-$Bi_2Mo_3O_{12}$ and γ-Bi_2MoO_6 in the temperature range of 400–550 °C [3,12]. Therefore, the oxidative dehydrogenation of *n*-butene over α-$Bi_2Mo_3O_{12}$ and γ-Bi_2MoO_6 catalysts at reaction temperatures in the range of 400–550 °C has been a subject of extensive study.

It was reported that a mixed catalyst composed of α-$Bi_2Mo_3O_{12}$ and γ-Bi_2MoO_6 showed a synergistic effect in

* Corresponding author. Tel.: +82 2 880 9227; fax: +82 2 889 7415.
E-mail address: inksong@snu.ac.kr (I.K. Song).

1381-1169/$ – see front matter © 2007 Elsevier B.V. All rights reserved.
doi:10.1016/j.molcata.2007.03.016

several selective oxidation reactions [13–16]. It was proposed that the synergistic effect of these two catalysts in the oxidative dehydrogenation of 1-butene was attributed to the formation of a crystal phase similar to β-$Bi_2Mo_2O_9$ [13]. A synergistic effect of α-$Bi_2Mo_3O_{12}$ and γ-Bi_2MoO_6 catalysts in the partial oxidation of propylene to acrolein has also been reported [14]. In the partial oxidation of propylene, the synergistic effect of these two catalysts was explained by a remote control mechanism, in which oxygen species formed on the γ-Bi_2MoO_6 migrate onto the surface of the α-$Bi_2Mo_3O_{12}$ to create active sites. Several plausible mechanisms have also been proposed to explain the synergistic effect of α-$Bi_2Mo_3O_{12}$ and γ-Bi_2MoO_6 catalysts [15,16].

Developing an efficient catalyst for the oxidative dehydrogenation of C_4 raffinate-3 to 1,3-butadiene would be a challenging work. Furthermore, elucidating the synergistic effect of α-$Bi_2Mo_3O_{12}$ and γ-Bi_2MoO_6 catalysts in the oxidative dehydrogenation of C_4 raffinate-3 would be worthwhile. In this work, α-$Bi_2Mo_3O_{12}$ and γ-Bi_2MoO_6 catalysts were prepared by a co-precipitation method for use in the oxidative dehydrogenation of C_4 raffinate-3 to 1,3-butadiene. The prepared catalysts were characterized by XRD, BET, FT-IR, Raman spectroscopy, and ICP-AES analyses. A series of mixed catalysts composed of α-$Bi_2Mo_3O_{12}$ and γ-Bi_2MoO_6 were then prepared by a mechanical mixing method, and were applied to the oxidative dehydrogenation of C_4 raffinate-3, in an attempt to investigate any synergistic effects of α-$Bi_2Mo_3O_{12}$ and γ-Bi_2MoO_6 catalysts. The oxygen mobility of the catalyst was measured by TPRO (temperature-programmed reoxidation) experiments, because oxygen mobility is known to a crucial factor determining the catalytic performance in the oxidative dehydrogenation of *n*-butene [2,17–22]. The adsorption ability of α-$Bi_2Mo_3O_{12}$ and γ-Bi_2MoO_6 for *n*-butene was measured by C_4 raffinate-3-TPD (temperature-programmed desorption) experiments.

2. Experimental

2.1. Catalyst preparation

The α-$Bi_2Mo_3O_{12}$ and γ-Bi_2MoO_6 catalysts were prepared by a co-precipitation method. A known amount of bismuth nitrate ($Bi(NO_3)_3{\cdot}5H_2O$ from Sigma–Aldrich) was dissolved in distilled water that had been acidified with concentrated nitric acid. The solution was then added dropwise into an aqueous solution containing a known amount of ammonium molybdate ($(NH_4)_6Mo_7O_{24}{\cdot}4H_2O$ from Sigma–Aldrich) under vigorous stirring. During the co-precipitation step, the pH of the mixed solution was precisely controlled using known amounts of ammonia solution (3 M). The pH values were maintained at 1.5 and 3.0 in the preparation of α-$Bi_2Mo_3O_{12}$ and γ-Bi_2MoO_6, respectively. After the resulting solution was vigorously stirred at room temperature for 1 h, the precipitate was filtered to obtain a solid product. The solid product was dried overnight at 110 °C, and it was then calcined at 475 °C for 5 h in a stream of air to yield the final form (α-$Bi_2Mo_3O_{12}$ and γ-Bi_2MoO_6). A series of mixed catalysts composed of α-$Bi_2Mo_3O_{12}$ and γ-Bi_2MoO_6 were also prepared by a mechanical mixing method. A mechanical mixture of α-$Bi_2Mo_3O_{12}$ and γ-Bi_2MoO_6 in different ratios was simply ground to prepare the mixed catalyst.

2.2. Characterization

The formation of α-$Bi_2Mo_3O_{12}$ and γ-Bi_2MoO_6 was confirmed by XRD (MAC Science, M18XHF-SRA), FT-IR (Nicolet, Impact 410), and Raman spectroscopy (Horiaba Jobin Yvon, T64000) measurements. The Bi/Mo atomic ratios of the prepared catalysts were determined by ICP-AES (Shimadz, ICP-1000IV) analyses. The surface areas of the catalysts were measured using a BET apparatus (Micromeritics, ASAP 2010).

The oxygen mobility of the catalyst was measured by TPRO (temperature-programmed reoxidation) experiments. Prior to the TPRO measurement, each catalyst was partially reduced by carrying out the oxidative dehydrogenation of C_4 raffinate-3 at 420 °C for 3 h in the absence of an oxygen feed. After placing the reduced catalyst in a conventional TPRO apparatus, a mixed stream of oxygen (10%) and helium (90%) was introduced to the catalyst sample. The furnace temperature was then increased from room temperature to 500 °C at a heating rate of 5 °C/min. The amount of oxygen consumed was measured using a thermal conductivity detector (TCD).

The adsorption ability of α-$Bi_2Mo_3O_{12}$ and γ-Bi_2MoO_6 for *n*-butene was measured by C_4 raffinate-3-temperature-programmed desorption (TPD) experiments. Each catalyst (2 g) was charged into the quartz reactor of a conventional TPD apparatus. The catalyst was pretreated at 200 °C for 2 h under a flow of helium (20 ml/min) to remove any physisorbed organic molecules. 20 ml of C_4 raffinate-3 (1-butene (14.2 wt.%) + *trans*-2-butene (38.3 wt.%) + *cis*-2-butene (20.0 wt.%) + *n*-butane (26.9 wt.%) + cyclobutane (0.4 wt.%) + methyl cyclopropane (0.1 wt.%) + residue (0.1 wt.%)) was then pulsed into the reactor every minute at room temperature under a flow of helium (5 ml/min), until the adsorption sites of the catalyst became saturated with *n*-butene. The physisorbed *n*-butene was removed by evacuating the catalyst sample at 50 °C for 1 h. The furnace temperature was increased from room temperature to 450 °C at a heating rate of 5 °C/min under a flow of helium (10 ml/min). The desorbed *n*-butene and other components were detected using a GC-MASS spectrometer (Agilent, 5975MSD-6890N GC).

2.3. Oxidative dehydrogenation of C_4 raffinate-3

The oxidative dehydrogenation of C_4 raffinate-3 to 1,3-butadiene was carried out in a continuous flow fixed-bed reactor in the presence of air and steam. C_4 raffinate-3 containing 72.5 wt.% *n*-butene (1-butene (14.2 wt.%) + *trans*-2-butene (38.3 wt.%) + *cis*-2-butene (20.0 wt.%)) was used as a *n*-butene source, and air was used as an oxygen source (nitrogen in the air serves as a carrier gas). Water was sufficiently vaporized by passing through a pre-heating zone and continuously fed into the reactor together with C_4 raffinate-3 and air. The feed composition was fixed at *n*-butene:oxygen:steam = 1:0.75:15. Prior to the catalytic reaction, the catalyst was pretreated with air at

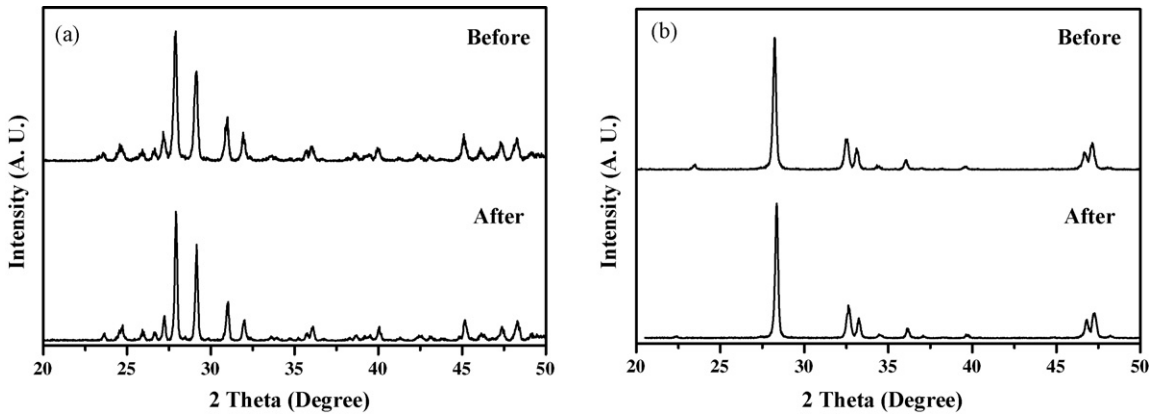

Fig. 1. XRD patterns of (a) α-$Bi_2Mo_3O_{12}$ and (b) γ-Bi_2MoO_6 catalysts obtained before and after the catalytic reaction (48 h-reaction at 420 °C).

470 °C for 1 h. The catalytic reaction was carried out at 420 °C. The gas hourly space velocity (GHSV) was fixed at 300 h^{-1} on the basis of *n*-butene. Reaction products were periodically sampled and analyzed with a gas chromatography. The conversion of *n*-butene and the selectivity for 1,3-butadiene were calculated on the basis of carbon balance as follows. The yield for 1,3-butadiene was calculated by multiplying conversion and selectivity.

$$\text{Conversion of } n\text{-butene} = \frac{\text{moles of } n\text{-butene reacted}}{\text{moles of } n\text{-butene supplied}}$$

$$\text{Selectivity for 1, 3-butadiene} = \frac{\text{moles of 1, 3-butadiene formed}}{\text{moles of } n\text{-butene reacted}}$$

3. Results and discussion

3.1. Formation of α-$Bi_2Mo_3O_{12}$ and γ-Bi_2MoO_6

The successful formation of α-$Bi_2Mo_3O_{12}$ and γ-Bi_2MoO_6 catalysts was well confirmed by XRD, FT-IR, Raman spectroscopy, and ICP-AES measurements. Fig. 1 shows the XRD patterns of α-$Bi_2Mo_3O_{12}$ and γ-Bi_2MoO_6 catalysts obtained before and after the catalytic reaction (48 h-reaction at 420 °C). These XRD patterns are in good agreement with those reported in previous works [2,18,23–25], indicating the successful formation of α-$Bi_2Mo_3O_{12}$ and γ-Bi_2MoO_6 catalysts. This also implies that the α-$Bi_2Mo_3O_{12}$ and γ-Bi_2MoO_6 catalysts are thermally stable during a catalytic reaction performed at 420 °C. FT-IR and Raman spectra of α-$Bi_2Mo_3O_{12}$ and γ-Bi_2MoO_6 catalysts are also in good agreement with those reported in previous works [2,23,24], although these are not shown here. The Bi/Mo atomic ratios of α-$Bi_2Mo_3O_{12}$ and γ-Bi_2MoO_6 determined by ICP-AES analyses were found to be 0.6 and 1.96, respectively. These values are in good agreement with the theoretical values (Bi/Mo = 2/3 for α-$Bi_2Mo_3O_{12}$ and Bi/Mo = 2 for γ-Bi_2MoO_6). The above results also support the conclusion that bismuth molybdate catalysts were successfully prepared. The BET surface areas of α-$Bi_2Mo_3O_{12}$ and γ-Bi_2MoO_6 catalysts were very low (1.9 and 3.5 m^2/g, respectively), as reported in previous works [18,26].

3.2. Catalytic performance and oxygen mobility

Fig. 2 shows the catalytic performance of α-$Bi_2Mo_3O_{12}$ and γ-Bi_2MoO_6 catalysts in the oxidative dehydrogenation of C_4 raffinate-3 at 420 °C after a 48 h-reaction. It was found that both the α-$Bi_2Mo_3O_{12}$ and γ-Bi_2MoO_6 catalysts exhibited a stable catalytic performance with time on stream without any catalyst deactivation during the 48 h-reaction, as can be inferred from the stable crystal structure of the catalysts before and after the reaction (Fig. 1). The conversion of *n*-butene and the selectivity for 1,3-butadiene obtained with γ-Bi_2MoO_6 catalyst were much higher than the corresponding values obtained with α-$Bi_2Mo_3O_{12}$ catalyst. As a consequence, the γ-Bi_2MoO_6 catalyst exhibited a higher yield for 1,3-butadiene than the α-$Bi_2Mo_3O_{12}$ catalyst.

In order to verify the different catalytic performance between α-$Bi_2Mo_3O_{12}$ and γ-Bi_2MoO_6, TPRO experiments were conducted with an aim of measuring the oxygen mobility of the catalysts. As mentioned earlier, the oxygen mobility of the bismuth molybdate catalyst plays a key role in catalytic performance in the oxidative dehydrogenation of *n*-butene [17–20]. It is expected that a bismuth molybdate catalyst with facile oxygen mobility would show an excellent catalytic performance in

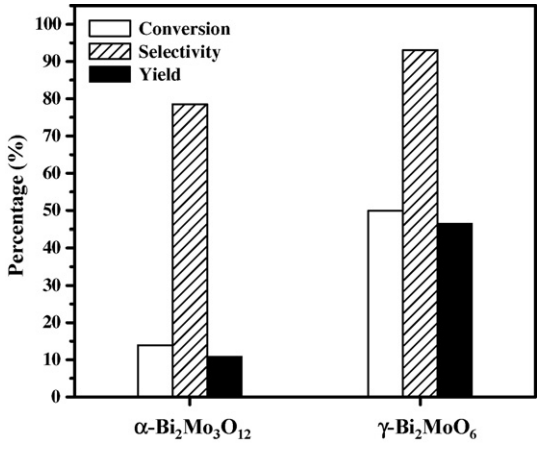

Fig. 2. Catalytic performance of α-$Bi_2Mo_3O_{12}$ and γ-Bi_2MoO_6 catalysts in the oxidative dehydrogenation of C_4 raffinate-3 at 420 °C after a 48 h-reaction.

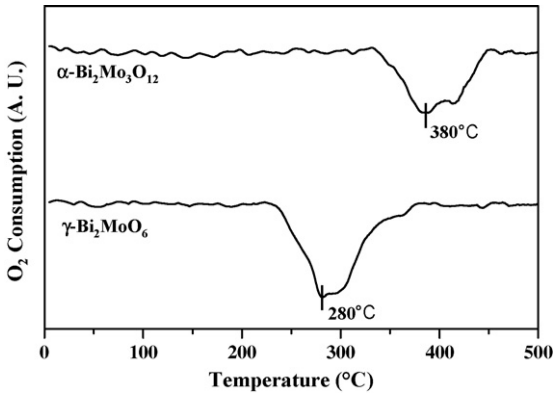

Fig. 3. TPRO profiles of partially reduced α-$Bi_2Mo_3O_{12}$ and γ-Bi_2MoO_6 catalysts.

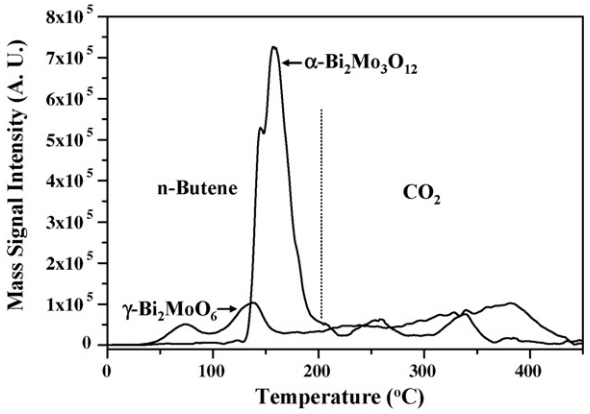

Fig. 5. C_4 raffinate-3-TPD profiles of α-$Bi_2Mo_3O_{12}$ and γ-Bi_2MoO_6 catalysts.

this reaction [19–22]. Fig. 3 shows the TPRO profiles of partially reduced α-$Bi_2Mo_3O_{12}$ and γ-Bi_2MoO_6 catalysts. TPRO peak temperature and TPRO peak area reflect the ease of oxygen mobility and the amount of make-up oxygen (oxygen vacancy), respectively. As shown in Fig. 3, the TPRO peak temperature for γ-Bi_2MoO_6 catalyst (280 °C) was much lower than that for α-$Bi_2Mo_3O_{12}$ catalyst (380 °C). Furthermore, the TPRO peak area for γ-Bi_2MoO_6 catalyst was larger than that for α-$Bi_2Mo_3O_{12}$ catalyst. These results indicate that the γ-Bi_2MoO_6 catalyst retains a higher oxygen mobility than the α-$Bi_2Mo_3O_{12}$ catalyst. It can thus be concluded that the enhanced catalytic performance of γ-Bi_2MoO_6 was due to the facile oxygen mobility of γ-Bi_2MoO_6.

3.3. Synergistic effect of α-$Bi_2Mo_3O_{12}$ and γ-Bi_2MoO_6

In order to investigate any synergistic effects of α-$Bi_2Mo_3O_{12}$ and γ-Bi_2MoO_6 on the catalytic performance in the oxidative dehydrogenation of C_4 raffinate-3, a series of mixed catalysts composed of α-$Bi_2Mo_3O_{12}$ and γ-Bi_2MoO_6 were prepared by a mechanical mixing method. Fig. 4 shows the catalytic performance of mixed catalysts in the oxidative dehydrogenation of C_4 raffinate-3 as a function of γ-Bi_2MoO_6 content. The selectivity for 1,3-butadiene increased monotonically with increasing γ-Bi_2MoO_6 content. It is interesting to note that the conversion of *n*-butene and the yield for 1,3-butadiene showed volcano-shaped curves with respect to γ-Bi_2MoO_6 content, indicating a synergistic effect of the α-$Bi_2Mo_3O_{12}$ and γ-Bi_2MoO_6 catalysts. The conversion of *n*-butene and the yield for 1,3-butadiene were the highest over the mixed catalyst composed of 10 wt.% α-$Bi_2Mo_3O_{12}$ and 90 wt.% γ-Bi_2MoO_6. The findings revealed that the crystal structure of the individual component in the mixed catalyst was not changed after the catalytic reaction under our experimental conditions. This indicates that the synergistic effect of α-$Bi_2Mo_3O_{12}$ and γ-Bi_2MoO_6 catalysts was not due to aggregation or segregation effects of these two components as a result of the formation of a new crystal phase.

Although the α-$Bi_2Mo_3O_{12}$ catalyst retained a lower oxygen mobility than the γ-Bi_2MoO_6 catalyst (Fig. 3), it is known that the α-$Bi_2Mo_3O_{12}$ catalyst has a favorable structure for providing abundant adsorption sites for *n*-butene [22], which leads to the facile activation of *n*-butene. In order to determine the adsorption ability of α-$Bi_2Mo_3O_{12}$ and γ-Bi_2MoO_6 catalysts for *n*-butene, C_4 raffinate-3-TPD experiments were conducted over the catalysts. Fig. 5 shows the C_4 raffinate-3-TPD profiles of α-$Bi_2Mo_3O_{12}$ and γ-Bi_2MoO_6 catalysts. It was found that

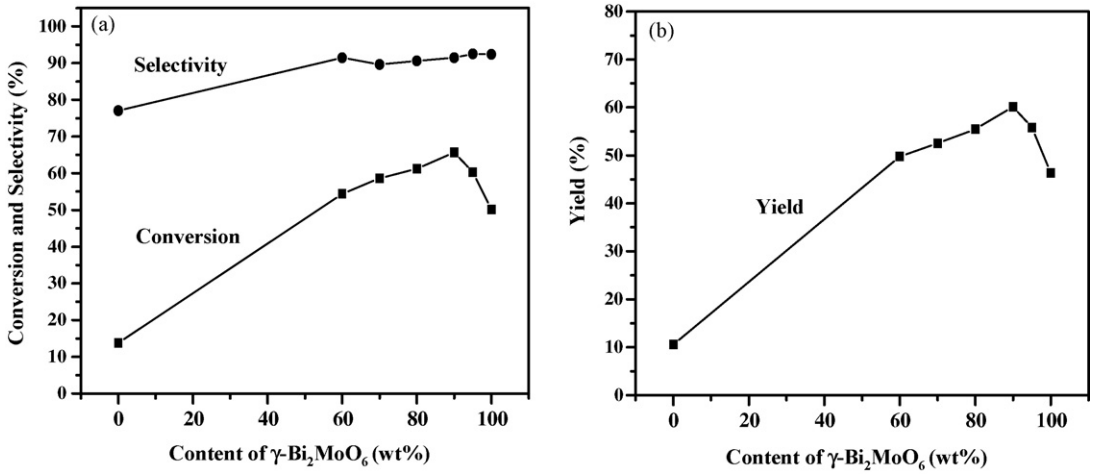

Fig. 4. Catalytic performance of mixed catalysts in the oxidative dehydrogenation of C_4 raffinate-3 as a function of γ-Bi_2MoO_6 content: (a) conversion of *n*-butene and selectivity for 1,3-butadiene, and (b) yield for 1,3-butadiene.

the α-$Bi_2Mo_3O_{12}$ catalyst showed strong mass signal intensities, while the γ-Bi_2MoO_6 catalyst showed weak mass signal intensities at temperatures ranging from room temperature to 450 °C. A series of TPD experiments revealed that the peaks in the low temperature region (below 200 °C) were attributed to desorbed *n*-butene (1-butene, *trans*-2-butene, and *cis*-2-butene), while those in the high temperature region (above 200 °C) corresponded to desorbed CO_2. The evolution of 1,3-butadiene was not detected over either catalyst under our experimental conditions. Undoubtedly, the total area of the TPD profile reflects the amount of *n*-butene adsorbed on the bismuth molybdate catalysts. As shown in Fig. 5, the total area of the TPD profile for the α-$Bi_2Mo_3O_{12}$ catalyst is much larger than that for the γ-Bi_2MoO_6 catalyst. This indicates that the α-$Bi_2Mo_3O_{12}$ catalyst retains abundant adsorption sites for *n*-butene, which leads to the facile activation of *n*-butene in the catalytic reaction.

It can be concluded that the γ-Bi_2MoO_6 catalyst retains a higher oxygen mobility than the α-$Bi_2Mo_3O_{12}$ catalyst, while the α-$Bi_2Mo_3O_{12}$ catalyst retains much more adsorption sites for *n*-butene than the γ-Bi_2MoO_6 catalyst. Therefore, it is believed that the synergistic effect of the α-$Bi_2Mo_3O_{12}$ and γ-Bi_2MoO_6 catalysts in the oxidative dehydrogenation of C_4 raffinate-3 was due to a combination of the facile oxygen mobility of γ-Bi_2MoO_6 catalyst and the abundant adsorption sites of α-$Bi_2Mo_3O_{12}$ catalyst for *n*-butene.

4. Conclusions

α-$Bi_2Mo_3O_{12}$ and γ-Bi_2MoO_6 catalysts were prepared by a co-precipitation method, and were applied to the oxidative dehydrogenation of C_4 raffinate-3 to 1,3-butadiene. The successful formation of α-$Bi_2Mo_3O_{12}$ and γ-Bi_2MoO_6 catalysts was well confirmed by XRD, FT-IR, Raman spectroscopy, and ICP-AES analyses. The γ-Bi_2MoO_6 catalyst exhibited a better catalytic performance than the α-$Bi_2Mo_3O_{12}$ catalyst due to the facile oxygen mobility of the γ-Bi_2MoO_6 catalyst. The conversion of *n*-butene and the yield for 1,3-butadine over the mixed catalysts showed volcano-shaped curves with respect to γ-Bi_2MoO_6 content due to the synergistic effect of the α-$Bi_2Mo_3O_{12}$ and γ-Bi_2MoO_6 catalysts. In particular, a mixed catalyst composed of 10 wt.% α-$Bi_2Mo_3O_{12}$ and 90 wt.% γ-Bi_2MoO_6 showed the best catalytic performance. It was revealed that the γ-Bi_2MoO_6 catalyst retained a higher oxygen mobility than the α-$Bi_2Mo_3O_{12}$ catalyst, while the α-$Bi_2Mo_3O_{12}$ catalyst retained much more adsorption sites for *n*-butene than the γ-Bi_2MoO_6 catalyst. It can be concluded that the synergistic effect of the α-$Bi_2Mo_3O_{12}$ and γ-Bi_2MoO_6 catalysts in the oxidative dehydrogenation of C_4 raffinate-3 was due to a combination of the facile oxygen mobility of γ-Bi_2MoO_6 and the abundant adsorption sites of α-$Bi_2Mo_3O_{12}$ for *n*-butene.

Acknowledgements

The authors acknowledge the support from Korea Energy Management Corporation (2005-01-0090-3-010).

References

[1] S.C. Oh, H.P. Lee, H.T. Kim, K.O. Yoo, Korean J. Chem. Eng. 16 (1999) 543.
[2] A.P.V. Soares, L.D. Dimitrov, M.C.A. Oliveira, L. Hilaire, M.F. Portela, R.K. Grasselli, Appl. Catal. A 253 (2003) 191.
[3] Ph.A. Batist, J.F.H. Bouwens, G.C.A. Schuit, J. Catal. 25 (1972) 1.
[4] R.K. Grasselli, Top. Catal. 21 (2002) 79.
[5] H.H. Kung, Adv. Catal. 40 (1994) 1.
[6] W.J. Linn, A.W. Sleight, J. Catal. 41 (1976) 134.
[7] M.F. Portela, M.M. Oliveira, M.J. Pires, Polyhedron 5 (1986) 119.
[8] D.A.G. Van Oeffelen, J.H.C. Van Hooff, G.C.A. Schuit, J. Catal. 95 (1985) 84.
[9] Ph.A. Batist, B.C. Lippens, G.C.A. Schuit, J. Catal. 5 (1966) 55.
[10] A.C.A.M. Bleijenberg, B.C. Lippens, G.C.A. Schuit, J. Catal. 4 (1965) 581.
[11] M. Egashira, K. Matsuo, S. Kagawa, T. Seiyama, J. Catal. 58 (1979) 409.
[12] J.C. Jung, H. Kim, A.S. Choi, Y.-M. Chung, T.J. Kim, S.J. Lee, S.-H. Oh, I.K. Song, J. Mol. Catal. A 259 (2006) 166.
[13] I. Matsuura, R. Shut, K. Hirakawa, J. Catal. 63 (1980) 152.
[14] Z. Bing, S. Pei, S. Shishan, G. Xiexian, J. Chem. Soc. Faraday Trans. 86 (1990) 3145.
[15] H.-G. Lintz, A. Quast, Catal. Lett. 46 (1997) 255.
[16] D. Carson, G. Coudurier, M. Forissier, J.C. Vedrine, A. Laarif, F. Theobald, J. Chem. Soc. Faraday Trans. 79 (1983) 1921.
[17] G.C.A. Schuit, J. Less Common Met. 36 (1974) 329.
[18] Ph.A. Batist, A.H.W.M. Der Kinderen, Y. Leeuwnburgh, F.A.M.G. Metz, G.C.A. Schuit, J. Catal. 12 (1968) 45.
[19] E. Ruckenstein, R. Krishnan, K.N. Rai, J. Catal. 45 (1976) 270.
[20] M.F. Porteal, Top. Catal. 15 (2001) 241.
[21] Y.M. Oka, W. Ueda, Adv. Catal. 40 (1994) 233.
[22] R.K. Grasselli, Handbook of Heterogeneous Catalysis, Wiley Publishing, New York, 1997.
[23] B. Grzybowska, J. Haber, J. Komorek, J. Catal. 25 (1972) 25.
[24] E.V. Hoefs, J.R. Monnier, G.W. Keulks, J. Catal. 57 (1979) 331.
[25] P. Boutry, R. Montarnal, J. Wrzyszcz, J. Catal. 13 (1969) 75.
[26] L.D. Krenzke, G.W. Keulks, J. Catal. 64 (1980) 295.